ORIGINAL PAPER

CrossMark

Fabrication of Engineered Silica-Functionalized-Polyanilines Nanocomposites for Water Decontamination of Cadmium and Lead

Mohamed E. Mahmoud[1] · Nesma A. Fekry[1]

Abstract

In this study, two novel functionalized silica nanocomposites were synthesized via covalent bonding with nanopolyaniline (NPANI) and crosslinked nanopolyaniline (CrossNPANI) to produce [NSi-NPANI] and [NSi-CrossNPANI], respectively. The two nanocomposites were portrayed by SEM, FT-IR, HR-TEM, BET-surface and TGA. The HR-TEM images of [NSi-NPANI] and [NSi-CrossNPANI] confirmed the particle size in the range 14.28–21.43 and 26.19–35.71 nm, respectively and these two nanocomposites were successfully applied to remove divalent cadmium and lead from solutions. As compared to nanosilica [NSi] sorbent, the maximum capacity values of the two nanocomposites for divalent cadmium and lead were identified to increase from 100–250 μmole g^{-1} (pH 1.0) to 750–800 μmole g^{-1} (pH 7.0) and from 400–1050 μmole g^{-1} (pH 1.0) to 650–1350 μmole g^{-1} (pH 6.0), at the optimum conditions. The adsorption data were compared using two and three parameter equations based on Langmuir, Freundlich, Temkin, Dubinin-Radushkevich, Redlish-Peterson and sips models. The kinetic study of [NSi-NPANI] and [NSi-CrossNPANI] revealed that the *pseudo*-second order kinetic was the best model to explain the kinetic data for cadmium(II) and lead(II). The free energy of sorption (ΔG^o), enthalpy (ΔH^o), and entropy (ΔS^o) changes were calculated to portend the nature of adsorption. Adsorptive extraction of toxic lead and cadmium from tap water and wastewater was successfully accomplished with the range of percentage recovery values 98.5–100.0 and 91.9–93.0%, respectively.

Keywords Nanopolyaniline · Nanosilica · Nanocomposites · Kinetic study · Adsorption isotherm models · Divalent cadmium and lead

Introduction

Heavy metal like lead and cadmium ions are generally discharged into the environment from different industrial activities including ceramics, pulp, metal finishing, lead smelters, mining, electroplating, battery industrialization and other activities [1–4]. The existence of these heavy metals in their ionic forms in water represents an extremely health hazard to human due to their persistence and non-biodegradability characters [5–7]. These toxic ions can permeate the human cell from water and foods causing severe clinical manifestations such as cancer, damage to the central nervous system, lung, brain and death [8]. Therefore, it is important to treat polluted water from metal ions before release and influx into the environment.

Adsorption technology is amongst several other well-known approaches commonly employed to extract metal ions from water [9]. The adsorption technique is listed as the best due to low cost, simple operation and high efficiency with the advantage of potential regeneration of the used sorbent [10]. The literature survey points to a plenty of applicable organic and inorganic sorbents in removal and water treatment of heavy metals. The inorganic sorbents are mainly including metal oxides (MOs) such as silicon, titanium, aluminum and iron oxides [11]. Chitosan, chitin, cellulose polymers and polyaniline (PANI) are examples of the organic sorbents [12]. Recently conducting polymers

✉ Mohamed E. Mahmoud
  memahmoud10@yahoo.com

  Nesma A. Fekry
  nesma.ahmedfekry@gmail.com

1 Chemistry Department, Faculty of Sciences, Alexandria University, P.O. Box 426, Alexandria 21321, Egypt

such (PANI) and nanopolyaniline (NPANI) as well as their composites have gained substantial interests due to outstanding performance with regard for metal sorption because of the existence of several functional groups, low cost, simple synthetic approaches [13]. PANI composites have been implemented as efficient sorbents for extraction of inorganic pollutants such as toxic metal ions from solutions [14].

For instance, A sol–gel method was described to synthesize polyaniline Sn(IV) tungstomolybdate and successfully used for removal of lead [15]. A composite was prepared using PANI/polypyrrole/hexagonal-mesoporous silica (PANI/PPy/HMS), characterized and investigated for cadmium adsorption and removal from solutions [16]. A sol–gel mixing procedure of (PANI) into Zr(IV) molybdophosphate (ZMP) was used to prepare polyaniline-Zr(IV) molybdophosphate (PAZMP) and the distribution of investigated metal ions indicated that this composite is substantially selective for nickel [17]. The sorption characteristics of cobalt ions from solutions by PANI/polypyrrole copolymer nanofibers were studied by the batch method and the removal efficiency was identified as 99.68% [18]. Removal of rubidium ion from solution was studied and explored using nanocomposite material of modified (PANI) with cobalt-prussian blue analogues (Co-PBA) [19]. Adsorptive removal of arsenic in different batch experiments was reported using novel synthesized nano-polyaniline/Fe^0 composite by reductive deposition of nano-Fe^0 onto the polyaniline nanofibers matrix at room temperature [20].

The implementations of PANI composites and derivatives as effective sorbents for removal of inorganic and organic pollutants from solutions have been also reported. For example, a chemical oxidative polymerization method was used to synthesize starch/PANI nanocomposite and subsequently tested for effective color removal of reactive violet 4 and reactive black 5 from solutions by the batch experiment [21]. A polymerization process was implemented to functionalize and coat polyaniline with Fe_3O_4 for the formation of (Fe_3O_4@PANI) composite in a simple two-step method and this material was employed to investigate the adsorptive removal reactions of naphthol derivatives and phenol from water samples [22]. PANI coated on lignocellulose composite was made via in-situ polymerization of aniline and used to adsorb reactive black 5 from solutions [23]. In addition, other polyaniline sorbents have been recently reported in the adsorption technique of different pollutants [24–27].

The adsorption isotherm data is an essential measure to calculate the adsorption performance by utilizing different model. Several two parameters isotherm models are generally used to explain the adsorption data including the Langmuir, Freundlich, Temkin and Dubinin-Radushkevich. On the other hand, three parameters isotherm models such as Redlish-Peterson, Sips, Toth and Khan are also employed [28–30]. Generally, that portend the isotherm constants for

an adsorption system and two processes are available. First is the linear method of isotherm data that is converting the isotherm equation to a linear form to find out the parameters. Second is the nonlinear method of isotherm data, which is subjected to their best accepting of the isotherm equation in its nonlinear form to the experimental result. However, depending on the linearization expression of the isotherm equation, the distribution of error changes either to the worst or to the superior [31]. Additionally, the linear regression method is not permanently a good option to apply for isotherms with more than two parameters. Therefore, several researchers have applied the method of nonlinear regression to evaluate the best accepting isotherm model. This approach is aimed to minimize the error distribution between the experimental adsorption data and the portend isotherm model. It has a particularity that the error distribution does not get altered as in linear regression method because all isotherm parameters are fixed on the same axis [32]. In addition, various error functions are utilized to estimate the isotherm data by nonlinear regression method. The most popular error functions are namely, the nonlinear Chi square test (X^2), the sum of the squares error (SSE), the average relative error (ARE), the sum of the absolute errors (EABS) and the hybrid fractional (HYBRID).

In this study, nanosilica (NSi) material was functionalized with nitrogen rich (NPANI) and (CrossNPANI) using formaldehyde for the formation of two novel nanocomposites, [NSi-NPANI] and [NSi-CrossNPANI]. The two functionalized nanocomposites were characterized and compared with (NSi) sorbent using SEM, FT-IR, TEM, TGA and surface area determination. In addition, the experimental data were manipulated to appraisal the nonlinear and linear regression isotherm, kinetics models and thermodynamics parameters. This work aims also to report the potential implementations of [NSi-NPANI] and [NSi-CrossNPANI] nanocomposites in the removal of cadmium and lead from solutions and different water specimens by the batch and multistage micro-column techniques in existence of diverse controlling parameters.

Experimental

Chemicals and Solutions

Silica gel nanoparticles (10–20 nm, specific surface area 140–180 m^2/g (BET) and assay 99.5%) were purchased from Aldrich Chemical Company, USA. Potassium persulphate (KPS) was purchased from Oxford, India (assay 98.9% and FW = 270.31). Aniline was obtained from Lobachemie, India. Aqueous solutions (0.1 mol L^{-1}) of metal ions were prepared in 1.0 L by dissolving the corresponding mass of the following salts. Anhydrous cadmium

chloride (assay 99.9% and FW 183.32) and lead acetate trihydrate (assay 99.99%, and FW 379.33) were purchased from BDH, UK, respectively. The concentrations of these metal ion solutions were analyzed by complexometric titration with 0.01 mol L^{-1} of EDTA (assay 99.0–101.0%, and FW 372.24) solution using the applicable buffer and indicator.

Instrumentations

Fourier transform infrared spectroscopic analysis (FT-IR) of NSi and nanocomposites were studied by a BRUKER Tensor 37. Thermal gravimetric analysis (TGA) of [NSi], [NSi-NPANI] and [NSi-CrossNPANI] were measured using a Perkin-Elmer TGA7 Thermobalance. The selected operating conditions are temperature heating range (20–800 °C), heating rate (10 °C min^{-1}), flow rate (20 mL min^{-1}) pure nitrogen atmosphere. Scanning electron microscope (SEM) JSM-5300-JEOL model and High resolution-transmission electron microscope (HR-TEM) JEM-2100 model were used to study the surface morphology and particle size of [NSi], [NSi-NPANI] and [NSi-CrossNPANI]. Surface area analysis of NSi and other nanocomposites were accomplished by using the BET method (Nova 3200 Nitrogen physisorption Apparatus, USA). The low concentration levels of divalent ions were measured by utilizing a Perkin Elmer flame atomic absorption spectrophotometer (PEFAAS), (model 2380).

Synthesis of NPANI and CrossNPANI

NPANI was prepared according to the following procedures. Aniline (7.0 mmol) was combined with 20.0 mL of distilled water (DW) and kept under stirring at room temperature (RT) for 10 min. This mixture was then maintained with stirring at 0–5 °C for 30 min. 7.0 mmol of potassium persulfate (KPS) was dissolved in 80 mL of DW and added as one portion to the aniline solution and stirred for another 1 h. This solution was kept at 0–5 °C to 24 h. The prepared polymer was collected, washed with DW and ethanol several times and dried under vacuum at 50 °C to produce the aimed material, NPANI. CrossNPANI was produced by heating NPANI at 180 °C for 3 h as previously described [33].

Synthesis of NSi-NPANI and NSi-CrossNPANI

The chemically attachment of NSi and NPANI was accomplished using formaldehyde. [NSi-NPANI] was prepared according to the following procedures. 2.0 g of NPANI was mixed with 10.0 mL of formaldehyde (CH_2O) and this mixture was heated with 3.0 mL of 1.0 mol L^{-1} of hydrochloric acid (HCl). 5.0 g of NSi was then added to this mixture and heated at 80 °C with continuous stirring for 2 h. The resulting material was left at RT for 12 h, collected, washed with ethanol several times and dried under vacuum at 70 °C until complete dryness. The possible structure of [NSi-NPANI] is represented in Scheme 1.
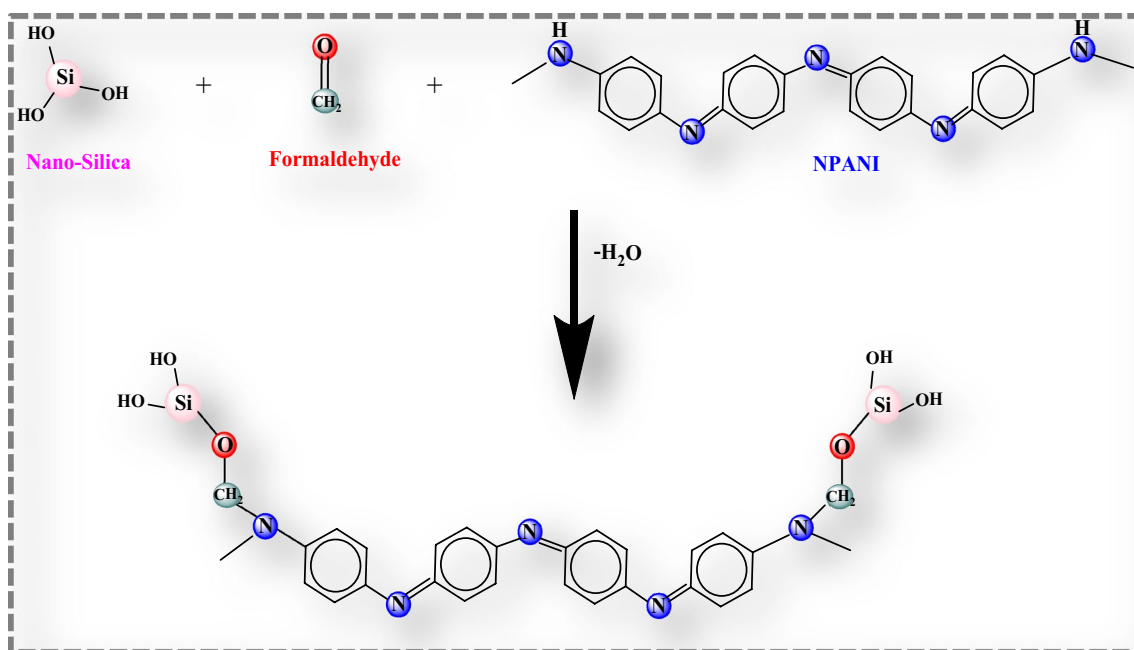
Scheme 1 The possible structure of [NSi-NPANI] nanocomposite
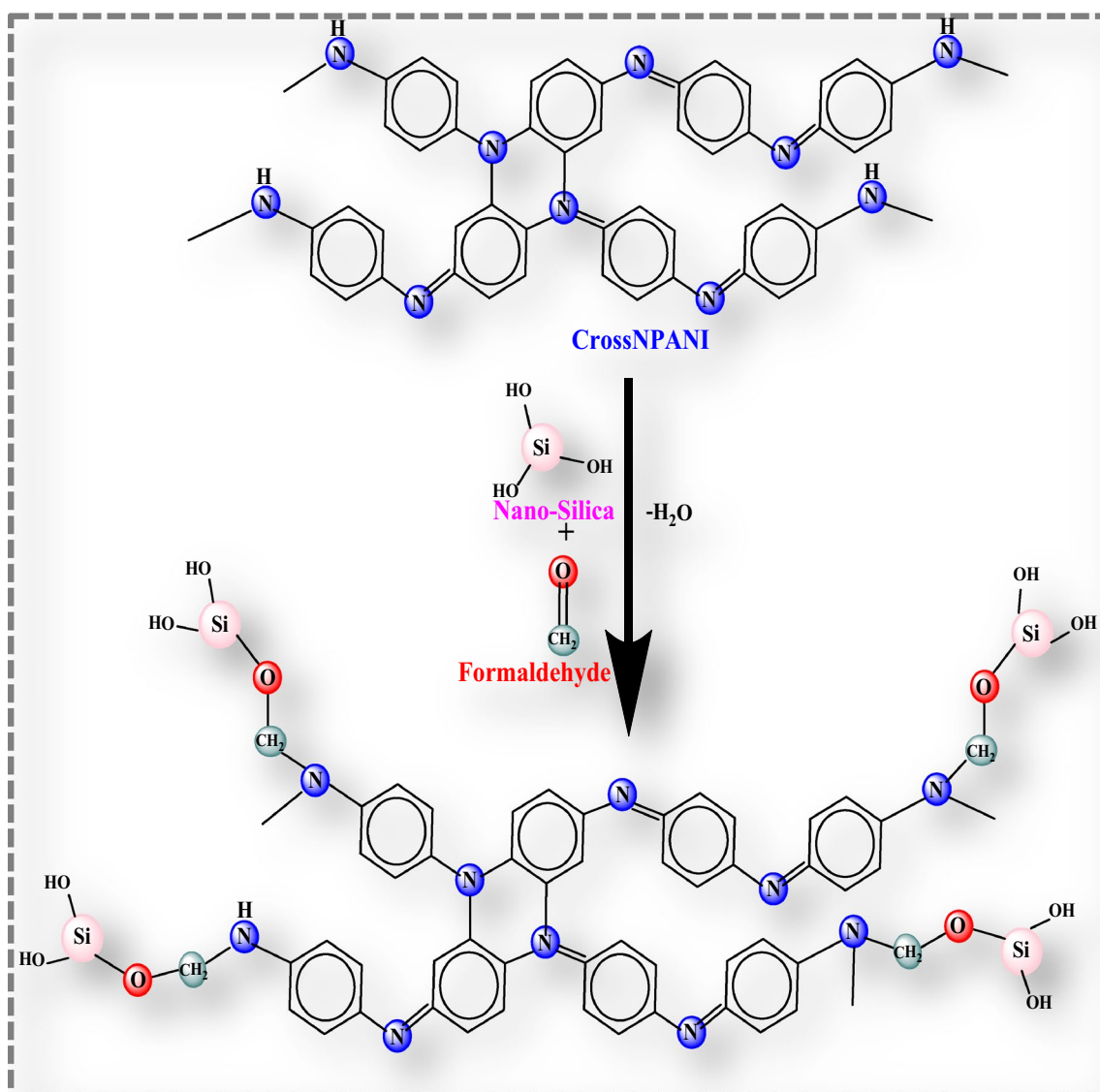
Synthesis of NSi-CrossNPANI

2.0 g of CrossNPANI was mixed with 10.0 mL of formaldehyde (CH_2O) and 3.0 mL of 1.0 mol L^{-1} of hydrochloric acid. This mixture was heated with stirring for 2 h in presence of 5.0 g of NSi at 80 °C. The resulting nanocomposite was left at RT for 12 h then collected, washed with ethanol several times and dried under vacuum at 70 °C until complete dryness. The possible structure of [NSi-CrossNPANI] is represented in Scheme 2.

Sorption Studies

Batch equilibrium method was performed to examine the availability of newly prepared and functionalized modified NSi for sorption and uptake of cadmium and lead ions. The influence of pH, contact time and starting metal concentration were studied according to the following procedures.

The Effect of pH

All batch sorption experiments were achieved at $(25 \pm 1 \ °C)$. Each experiment was performed in a 50 mL volumetric flask by combining a 1.0 mL of 0.1 mol L^{-1} metal ion solution

Scheme 2 The possible structure of [NSi-CrossNPANI] nanocomposite

with 10 ± 1 mg of the selected NSi, [NSi-NPANI] or [NSi-CrossNPANI] nanocomposite and adding 9.0 mL of acidic or neutral buffer solution (pH 1.0–7.0). The mixture was shaken by an automatic shaker for 30 min then separated by filtration and washed with 50 mL of DW. The remaining metal ions were measured by EDTA titrations and each experiment was duplicated several times. The sorption capacity value was calculated by Eq. (1).

$$q = \frac{(C_0 - C)V}{m} \times 10^3 \qquad (1)$$

where, C_o and C (mol L^{-1}) are the starting and remaining metal ion concentration, respectively, V is the volume of the sorption reaction in mL, m is the mass of dry a nanocomposite in gram and q (µmol g^{-1}) is the metal sorption capacity that represents the quantity of metal ion (µmol) adsorbed per gram of NSi, [NSi-NPANI] or [NSi-CrossNPANI] nanocomposite (Scheme 3).

Effect of Contact Time

The previously characterized batch experiment was accomplished using various shaking times (1, 5, 10, 15, 20, 25 and 30 min) at optimum buffering status of each metal sorption. A 1.0 mL of divalent metal ion (0.1 mol L^{-1}) solution was mixed with 10 ± 1 mg of [NSi-NPANI] or [NSi-CrossNPANI] followed by adding (9.0 mL) of the optimum buffer and shaken by an automatic shaker for the selected period of time. The separated metal ions by filtration were washed with 50 mL of DW. The metal sorption capacity was calculated by duplication the steps as before.

Sorption Isotherm

In this study, the sorption equilibrium of ions onto [NSi-NPANI] and [NSi-CrossNPANI] was analyzed as a function of ion concentration (0.01–0.2 mol L^{-1}). The divalent ion solution was combined with 9.0 mL of the optimum buffer conditions solution. A 10 ± 1 mg of the modified NSi was added to this mixture and automatically shaken for 30 min. The mixture was filtered and washed three times with 50 mL
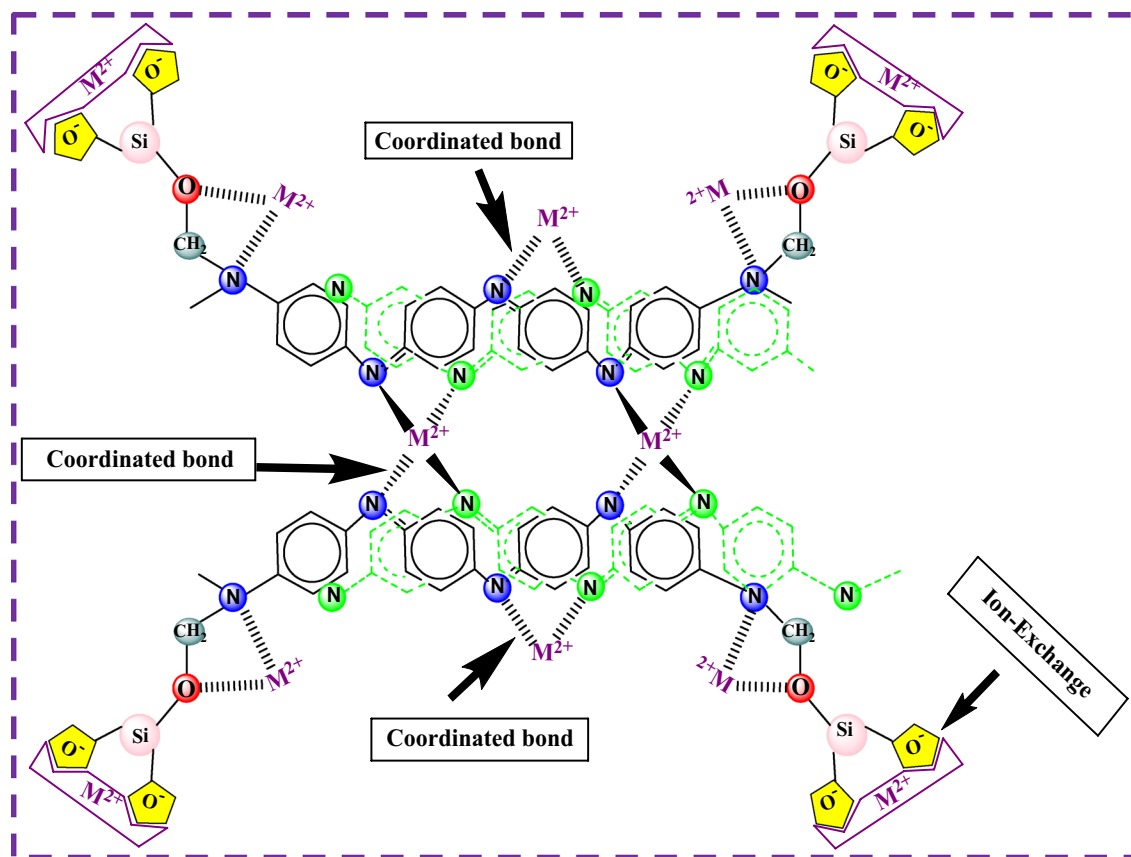
Scheme 3 Metal binding with [NSi-NPANI] nanocomposite

of DW. The remaining concentration of ion was measured by EDTA titrations and the metal sorption capacity data were calculated on the basis of triplicate analysis. The sorption isotherm results were examined by utilizing six various isotherm models: Four two-parameter sorption isotherm models as Langmuir, Temkin, Dubinin-Radushkevich (D-R), Freundlich and two three-parameter sorption isotherm models as Sips and Redlich-Peterson (R-P).

Thermodynamic Study

The sorption experiments were performed at temperature values 293, 303, 313, and 323 K to determine the thermodynamic parameters (ΔG^o, ΔH^o, ΔS^o) according to the next steps. A 1 mL solution of divalent ion (cadmium or lead) of known starting concentration (0.01–0.2 mol L^{-1}) was mixed with 10 ± 1 mg of [NSi-NPANI] or [NSi-CrossNPANI] and 9.0 mL of the optimum buffer condition for each metal ion. This mixture was shaken at the chosen temperature for 30 min and the remaining concentration of divalent ions was determined as illustrated above.

Adsorptive Removal of Metal Ions from Different Water Samples

Various water specimens (tap water, sea water and industrial wastewater from AL-Nubariya canal) were collected and utilized to calculate the efficiency of NSi and modified NSi for extraction of two divalent ions. Three water specimens were collected and spiked with cadmium or lead ions and 1 L of each sample was passed over a micro-column system packed with 100.0 ± 1.0 mg of NSi, [NSi-NPANI] or [NSi-CrossNPANI] under air pressure and flow rate of 10 mL min^{-1}. The effluent solution was estimated by atomic absorption analysis (AAA). This procedure was reiterated several times and the average percentage values (%E) of extracted metal ion were calculated according to Eq. (2).
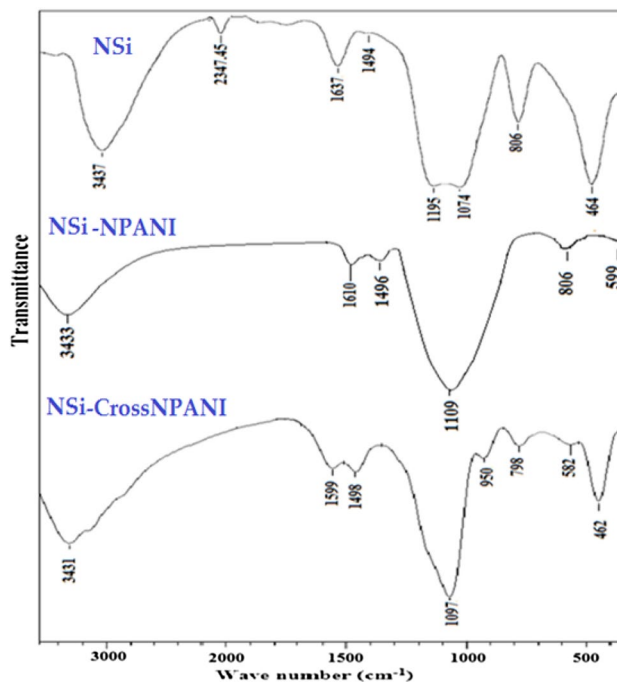
$$\%E = \frac{(C_0 - C)}{C_0} \times 100 \qquad (2)$$

where, C_o and C (mg L^{-1}) are the starting and eventual divalent ion concentration, respectively.

Result and Discussion

Characterization

The FT-IR spectra of [NSi], [NSi-NPANI] and [NSi-CrossNPANI] are represented in Fig. 1. Several characteristic

Fig. 1 FT-IR spectra of [NSi], [NSi-NPANI] and [NSi-CrossNPANI] nanocomposites

bands in the range 3423–3439 cm^{-1} are characterized and mainly due to the presence of different symmetrical stretching modes of functional groups such as amine (N-H) and hydroxyl (OH). The FT-IR spectrum of [NSi] exhibited some characteristic peaks which are related to hydroxyl groups on the surface (Si-OH) at 3437 cm^{-1}, asymmetric stretching of Si-O-Si at 1074 cm^{-1}, symmetric stretching at 806 cm^{-1}, and bending at 462 cm^{-1}. The obtained peak at 2347 cm^{-1} may be assigned to (Si-H) group [34]. The FT-IR spectrum of modified nanocomposite, [NSi-NPANI] is also shown in Fig. 1. The FT-IR spectrum of [NSi-NPANI] exhibited several characteristic peaks such as C=N and C=C bonds at 1610 and 1496 cm^{-1} which are also related to the quinonoid and benzenoid structures, respectively. The observed wide peak at 1109 cm^{-1} is fundamentally due to (Si-O-C-). Moreover, the vibrational bands at 470, 615 and 808 cm^{-1} overlap together to give two small bands at 806 and 599 cm^{-1} due to the conversion of (-NH-) into (-N-C-) by the crosslinker (formaldehyde CH_2O) [35]. The FT-IR spectrum of [NSi-CrossNPANI] refers to the opening of the quinone due to the peak at 1599 cm^{-1} and shorter compared to the benzenoid band at 1498 cm^{-1}. The weak intense peak of Si-O-C and Si-OH bonds and their shifts to 1097 and 3431 cm^{-1}, respectively are mainly produced as a result of coating silica with Cross NPANI.

The TGA data of [NSi], [NSi-NPANI] and [NSi-CrossN-PANI] were also studied and evaluated. The TGA of [NSi] was found to refer to the existence of only one degradation

step at the temperature < 477.1 °C. The % loss of this degradation step was found as 1.371% due to desorption of some adsorbed H_2O molecules from the surface of [NSi] and this indicates that [NSi] sorbent is highly stable in the studied temperature range of 50–800 °C. The TGA-thermogram of [NSi-NPANI] nanocomposite is clearly referring to the existence of three successive thermal degradation steps. The first decomposition was produced in the temperature range 28.1–79.2 °C that is related to desorption of surface loaded water molecules and the identified percentage loss of this step is 4.035%. The second decomposition step is mainly focused on the temperature range 79.2–497.7 °C with a percentage loss corresponding to 11.061%. The third decomposition step is focused on the temperature range 497.7–732.7 °C with a percentage loss corresponding to 15.843%. The second and third decomposition steps are generally produced by the facile thermal decomposition of the loaded organic molecule, NPANI, from the surface. The total percentage loss of NPANI from [NSi-NPANI] is 26.904% and this value refers to the loaded amount of NPANI on this nanocomposite. The TGA of [NSi-CrossNPANI] nanocomposite was found also to produce three major degradation steps. The first thermal decomposition step is identified at temperature < 128.9 °C with 13.317% loss due to desorption of some adsorbed H_2O molecules from the surface of this crosslinked nanocomposite. The second and third thermal decomposition steps were characterized at temperature < 417.4 and 647.4 °C with the percentage loss values of 8.383 and 28.906%, respectively. The total degradation of loaded CrossNPANI from the surface of [NSi-CrossNPANI] can be deduced as 37.289%.

The surface morphology and imaging of [NSi], [NSi-NPANI] and [NSi-CrossNPANI] nanocomposites are represented in Fig. 2. These images confirm that nanosilica exhibited regular and homogenous shape. However, the SEM-image of [NSi-NPANI] nanocomposite is brighter and smoother than the image of [NSi] and this gives a good evidence for the surface coating of silica with the target material. The SEM-image of [NSi-CrossNPANI] nanocomposite is also brighter and smoother than other nanocomposites. Finally, all of these observations prove the success of crosslinking of NPANI and CrossNPANI on nanosilica matrix.

In addition, the TEM images of [NSi], [NSi-NPANI] and [NSi-CrossNPANI] are shown in Fig. 2 at magnification orders of 60,000. It is evident that the particles are formed in aggregates in a linked shape. The detected range of particle size of [NSi-NPANI] was characterized as 14.28–21.43 nm, while that of [NSi-CrossNPANI] was found in the range 26.19–35.71 nm.

The surface area determination of [NSi], [NSi-NPANI] and [NSi-CrossNPANI] nanocomposites was also performed using the multipoint BET method. [NSi] sorbent was found to exhibit a large surface area according to the multipoint BET method by giving 2.126×10^2 m^2 g^{-1}. The pore volume and pore size values of [NSi] sorbent were found to correspond to 3.730×10^{-1} cc g^{-1} and 9.620 Å, respectively. The [NSi-NPANI] was found to show a large surface area according to the multipoint BET method as 2.458×10^2 m^2 g^{-1}. However, the pore volume and pore size values of [NSi-NPANI] were identified as 3.630×10^{-1} cc g^{-1} and 9.664 Å, respectively. Finally, the [NSi-CrossNPANI] was found to show a large surface area according to the multipoint BET method as 1.438×10^2 m^2 g^{-1}. The pore volume and pore size values were characterized as 2.902×10^{-1} cc g^{-1} and 8.544 Å.

Sorption Studies

Effect of pH

The pH of aqueous metal ion solution is well known as an important factor in the sorption process by different sorbents [36–38]. The effect of pH on sorption processes of cadmium and lead by the newly designed and functionalized [NSi-NPANI] and [NSi-CrossNPANI] nanocomposites were studied and compared with [NSi] using the pH range from 1.0 to 7.0 at 25 °C. Table 1 compiles the collected metal sorption capacity values of cadmium and lead. The collected data indicate that [NSi-NPANI] and [NSi-CrossNPANI] are superior to [NSi] in the process of adsorptive removal of the investigated metal ions in all evaluated pH values. The two functionalized [NSi-NPANI] and [NSi-CrossNPANI] nanocomposites are regarded as a combination of different functional groups that are capable of pointing diverse coordination complexes and/or ion exchange reaction with metal ions. The functional groups accountable for binding with the target divalent metal ions are generally in the form of the amine (-NH) and hydroxyl (-OH). The results of this study refer to the general rule whereas, the higher pH, the high degree of these functional groups deprotonation will be and hence the larger numbers of negative binding positions are directed towards metal ion interaction [39]. The maximum metal capacity values of cadmium and lead were found to agree to 1000 µmol g^{-1} (pH 6.0) and 1350 µmol g^{-1} (pH 6.0) µmol g^{-1} using [NSi-CrossNPANI], respectively. In the same way, the maximum metal capacity values of cadmium and lead were found to correspond to 750 and 800 µmol g^{-1} using [NSi-NPANI], respectively at pH 7.0. Otherwise, [NSi] exhibited the metal sorption capacity values of cadmium and lead as 400 and 500 µmol g^{-1}, respectively at pH 7.0. Therefore, the order of metal capacity of the investigated and evaluated metal ions by the newly designed silica nanocomposites can be listed in the following order: [NSi-CrossNPANI] > [NSi-NPANI] > [NSi].

Fig. 2 SEM and HR-TEM images of **a** [NSi], **b** [NSi-NPANI] and **c** [NSi-CrossN-PANI]
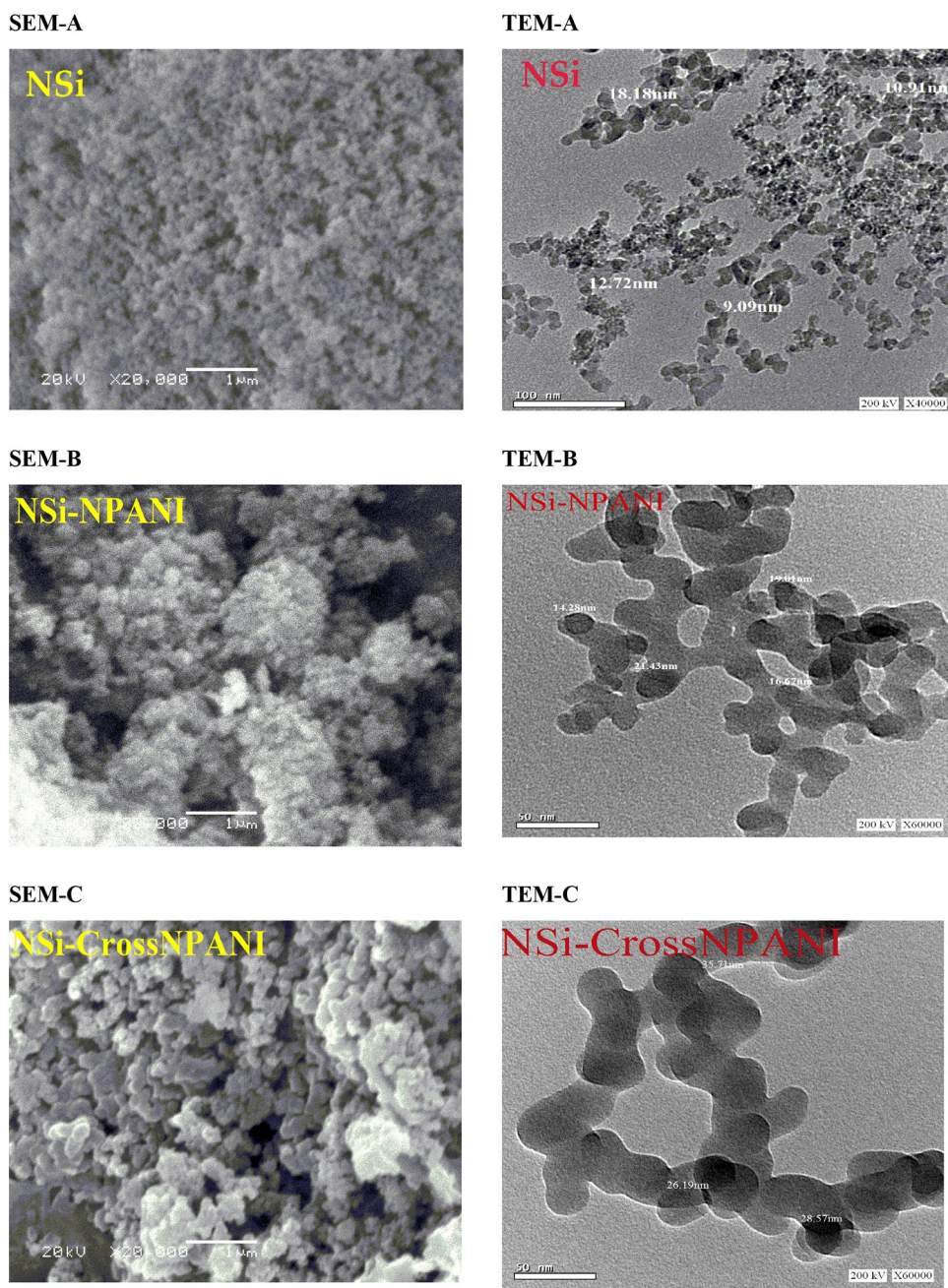
Table 1 Effect of pH on sorption capacity values of different metal ions

Nanosorbent	Metal ion	Metal capacity expressed in (μmole g^{-1})						
		pH						
		1	2	3	4	5	6	7
NSi	Cd(II)	66.7	100	150	200	266.7	400	400
	Pb(II)	350	350	400	400	400	500	500
NS-NPANI	Cd(II)	100	150	250	300	350	500	750
	Pb(II)	400	400	450	450	650	650	800
NSi-CrossNPANI	Cd(II)	250	500	650	700	750	1000	800
	Pb(II)	1050	1200	1250	1300	1300	1350	1200

Effect of Shaking Time

The effect of time on sorption processes of cadmium and lead by [NSi-NPANI] and [NSi-CrossNPANI] is shown in Fig. 3, respectively and this controlling parameter was studied by the batch technique using different shaking time intervals in the regulating time from 1 to 30 min. All metal ions were found to display a general trend in which the sorption process reaches a maximum value with the increase in contact time from 1 to 15 min. This step involves a rapid elevate in the metal sorption capacity of the metal ions onto nanocomposites owing to the abundant and availability of active binding sites on the surface. After 15 min, with the gradual occupancy of these positions, the metal ions sorption becomes less efficient leading to reach maximum sorption at 30 min [40]. The maximum sorption capacity values of cadmium by [NSi-NPANI] and [NSi-CrossNPANI] were 750 and 1000 μmol g^{-1}, respectively. Finally, the equilibrium time for maximum sorption capacity value of lead by [NSi-NPANI] and [NSi-CrossNPANI] identified as 800 and 1300 μmol g^{-1} at 30 min, respectively.

Adsorption Equilibrium of [NSi-NPANI] and [NSi-CrossNPANI] by Different Models

The adsorption isotherm recognizes how the quantity of molecules are suspended between the solid and liquid phase when the adsorption operations reach balance. It portends important information about the main mechanisms included in the extraction of divalent ions such cadmium and lead when reacting with the nanocomposite such as newly designed [NSi-NPANI] and [NSi-CrossNPANI] nanocomposites. Therefore, the equilibrium adsorption operations were determined in terms of divalent ion concentration. The isotherm equilibrium data were investigated using six various adsorption isotherm models focused on four 2-parameter models as Langmuir, Freundlich, Dubinin-Radushkevich (D-R), Temkin, and two 3-parameter models as Redlich-Peterson and Sips. The equations representing theses six models are compiled in Table S1 (Supplementary materials).

The Langmuir isotherm theory supposes the monolayer of adsorbate molecules surrounding a homogeneous adsorbent surface where all adsorption sites are found to be analogous and energetically tantamount. The Freundlich isotherm model is generally used to depict the adsorption for multilayers on a heterogeneous adsorbent surface in the solution. Apart from these, the D-R model is usually applied to recognize between the physical and chemical adsorption processes of metal ions. Finally, the Temkin isotherm model supposes that the reduction in the heat of adsorption is linear and its derivation is characterized by a uniform distribution of binding energies [28].

The Redlich-Peterson isotherm model combines elements from both the Langmuir and Freundlich isotherms and amends the inaccuracies. Also, it can be utilized either in homogenous or heterogeneous systems. Whereas the Sips model is combined from the Freundlich and Langmuir models. At a low concentration of divalent ions, this model is reduced efficacious to the Freundlich isotherm. It prognosticates a monolayer sorption capacity, which is characteristic of the Langmuir isotherm [28].

The nonlinear optimization method has been accomplished to determine the superior fit of different two- and three-parameters adsorption models. The optimization operation needs an error function that able to estimate the acceptance of the isotherm model to the experimental equilibrium data. In this study, five various error functions were investigated by minimizing the particular error function across the concentration range studied, using the *"SOLVER ADD-IN"* with Microsoft's spreadsheet [31, 41]. The error functions used in this paper are presented in Table S2 (Supplementary materials).

Figure 4 illustrates the isotherm equilibrium adsorption of cadmium and lead by newly designed [NSi-NPANI] and [NSi-CrossNPANI] nanocomposite using nonlinear analysis of Langmuir, Temkin, R-P, Freundlich, D-R and Sips. The data were fitted with Langmuir isotherm equation and the results are summarized in Tables 2, 3 and S3 (Supplementary materials). The correlation coefficients (R^2) were calculated in order to compare the linear and nonlinear regression analysis results. As listed in Table 2, high correlation coefficients were derived and identified by fitting experimental

Fig. 3 Effect of contact time on using [NSi-NPANI] and [NSi-CrossNPANI]
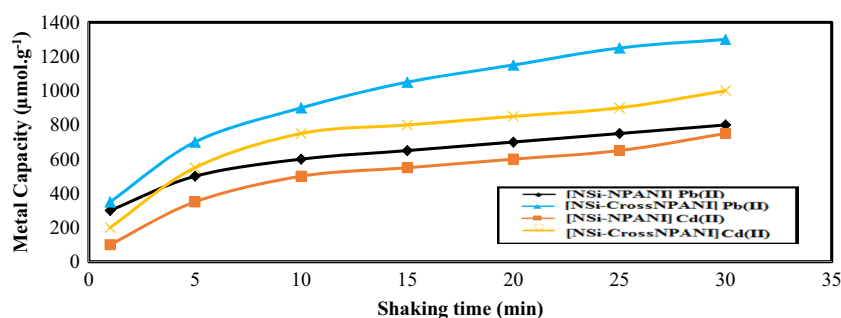
Table 2 Isotherm parameters and error obtained by nonlinear fitting (two-parameter isotherm models) using [NSi-NPANI]

Model isotherm	Constants with error analysis	Metal ion	
		Cadmium	Lead
Langmuir	q_{max} (mg g^{-1})	118.000	210.4221264
	K_L (L mg^{-1})	1.79×10^{-4}	7.8158×10^{-5}
	R^2	0.9973	0.9972
	SE	5.52293297	1.52708
	RMSE	17.48257	37.80004
	NSD	24.1105	36.11823
	ARE	16.494117	29.11615
	EBAS	74.54074	171.0098
	HYBRID	464.9313	1311.724
	X^2	18.73149	54.73646
Freundlich	K_F (L mg^{-1})	3.82×10^{-1}	5.56×10^{-2}
	n	1.69	1.25
	R^2	0.9393	0.9193
	SE	4.669891	6.802873
	RMSE	12.53703	17.27293
	NSD	18.62996	12.6863
	ARE	14.61133	11.11521
	EBAS	59.22923	89.23099
	HYBRID	266.3269	235.6412
	X^2	10.63769	10.65762
Temkin	b_T	67.37268	33.25467
	A_T (L mg^{-1})	1.000219	1.000098
	R^2	0.8485	0.8821
	SE	3.43322	10.30645
	RMSE	28.4021	21.14984
	NSD	38.49043	23.57764
	ARE	33.93589	19.42381
	EBAS	143.2181	107.0122
	HYBRID	1068.257	456.2934
	X^2	70.89157	28.55848
Dubinin-Radushkevich	q_s (mg g^{-1})	101.4212	187.4758
	K_{ads} (mol^2/KJ^2)	0.264658	1.003492
	R^2	0.7772	0.7994
	SE	6.455932	8.712759
	RMSE	39.85276	68.15699
	NSD	113.1853	90.77685
	ARE	79.08476	71.26846
	EBAS	216.5116	335.0056
	HYBRID	4632.0888	6293.689
	X^2	104.2818	172.4171

data into the Langmuir model (0.9973), (0.9972) for cadmium and lead onto [NSi-NPANI], respectively, as compared with other models. The data in Table S3 refers to the highest R^2-values using Langmuir model (0.9734) and (0.9976) for cadmium and lead onto [NSi-CrossNPANI], respectively.

The maximum sorption capacity values (q_{max}) of lead and cadmium may be explicated on the basis different selectivity of metal ions to the surface functional groups. The q_{max} values using Langmuir model were 118.0000000 and 210.4221264 mg g^{-1} for cadmium and lead, respectively. These values are very close to the experimental metal capacity data, which indicates that the Langmuir model provides a good example for the sorption of lead and cadmium onto [NSi-NPANI] and [NSi-CrossNPANI].

The R^2 values of lead using the evaluated isotherms confirm the follows sequence. Lead onto [NSi-NPANI] follows Langmuir (best fit) > Sips > Redlich-Peterson > Freundlich > Temkin > Dubinin-Radushkevich. On the other hand, lead onto [NSi-CrossNPANI] follows Langmuir(best fit) > Sips > Freundlich > Redlich-Peterson > Temkin > Dubinin-Radushkevich.

The linear isotherm parameters of cadmium and lead by [NSi-NPANI] and [NSi-CrossNPANI] nanocomposites are shown in Table 4. The adsorption isotherm studies obviously indicate that the adsorptive attitude of divalent ions satisfies not only the Langmuir assumptions but also the sips assumptions based on the high values of correlation coefficients as 0.9651 and 0.977 for cadmium onto [NSi-NPANI] and [NSi-CrossNPANI], respectively. These values indicate that the sorption of the lead onto two previously nanocomposites were fitted well for the Langmuir model. The Sips adsorption isotherm model equation is depicted by the dimensionless heterogeneity factor, n that can likewise be used to characterize the system's heterogeneity when n is between 0 and 1 or close to unity. The heterogeneity factor (n) values were identified as 0.99 and 0.56 for cadmium onto the two modified nanocomposites. Therefore, the Sips equation was converted to the Langmuir equation to describe the preferential binding of metals on all sites of nanocomposites as homogeneous surfaces. In addition, a relationship between heterogeneity and affinity factors is expected. Therefore, the affinity of cadmium ions increased and were facilely adsorbed by the available donor atoms on the nanocomposites. Finally, it is significant to record that the calculated R^2 values by linear analysis methods were all fewer than the corresponding R^2 values obtained by nonlinear analysis methods.

Adsorption Kinetic Studies

The kinetic studies for adsorptive behaviors of cadmium and lead ions by [NSi-NPANI] and [NSi-CrossNPANI] nanocomposites were investigated by utilizing four models; the *pseudo*-first, *pseudo*-second-order, intra-particle diffusion and Elovich models. The k_1, q_e, K_2, K_{id}, C, α and β factors were calculated and compiled in Table 5 and the correlation

NSi-NPANI

(A) Pb(II)

NSi-CrossNPANI

Pb(II)

(B) Cd(II)

Cd(II)
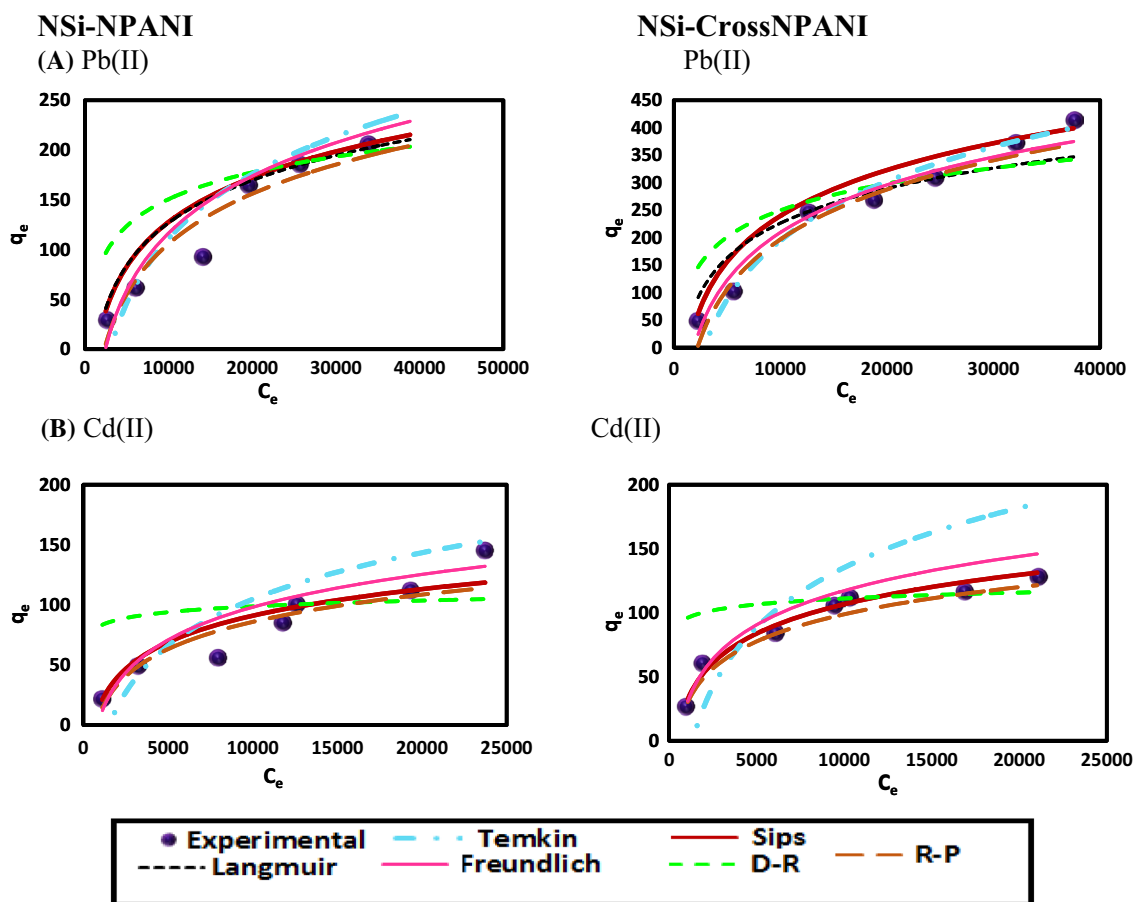
Fig. 4 Adsorption isotherms of metal ions by different models

coefficients obtained from these plots are listed in Table S4 (Supplementary materials).

The *pseudo*-first order kinetic constants for the adsorption of lead and cadmium on [NSi-NPANI] and [NSi-Cross-NPANI] obtained from the slope and the intercept of the linear relevance $\ln(q_e - q_t)$ on y-axis and time (t) on x-axis in Table 5. The correlation coefficient value for the *pseudo* first-order model kinetic model cadmium was found to correspond to 0.9717 and 0.9847 onto [NSi-NPANI] and [NSi-CrossNPANI], respectively. The k_1 value of the *pseudo*-first order was found 7.95×10^{-2} and 7.16×10^{-2} min^{-1} for cadmium onto [NSi-NPANI] and [NSi-CrossNPANI], respectively. The correlation coefficient value for lead was found to correspond to 0.9845 and 0.9607 onto [NSi-NPANI] and [NSi-CrossNPANI], respectively. The R^2 value of two divalent ions using the *pseudo* first-order model is smaller than the R^2 values in other models, refer to this model is inapplicable. It was likewise indicated in the existent work that q_e values are lower than q_e from *pseudo*-second order model. This indicates that *pseudo*-first order equation might not be adequate to consture the mechanism of cadmium and lead onto the two modified nanocomposites interactions.

The straight-line plots using the *pseudo*-second order model between t/q_t versus time (t) for sorption of the two investigated divalent ions are clarified in Fig. 5. The intercept and slope were used to determine two parameters (q_e and K_2) values, respectively. The *pseudo* second-order model is considered and confirmed as the rate-limiting step for the forming of chemisorptive bond of divalent ions via exchange or sharing of electrons. The R^2 values of the *pseudo*-second order kinetic model were obtained as 0.9879 and 0.9915 for lead and cadmium ions onto [NSi-CrossN-PANI], respectively. A high correlation coefficients for lead and cadmium were identified as 0.9887 and 0.9827 using [NSi-NPANI], respectively. The calculated equilibrium adsorption capacity values, q_e, were found to correspond to 303.03 and 125.00 mg g^{-1} for lead and cadmium on [NSi-NPANI], respectively. These results were superior than those related to the *pseudo*-first order model, indicating that the uptake operation of cadmium and lead followed *pseudo*-second order expression.

The intraparticle diffusion constants for sorption of cadmium and lead onto [NSi-NPANI] and [NSi-CrossNPANI] are calculated and compiled in Table 5. The plots may

Model isotherm	Constants and error function	Nanocomposite	Metal ion Cadmium	Lead
Redlish-peterson	K_R (L g^{-1})	NSi-NPANI	0.490756	0.97666
		NSi-CrossNPANI	1.285547	0.168367
	a_R (L mg^{-1})	NSi-NPANI	0.854668	13.638583
		NSi-CrossNPANI	0.654078	1.094016
	b_R	NSi-NPANI	0.464292	0.23504
		NSi-CrossNPANI	0.578672	0.24214
	R^2	NSi-NPANI	0.8567	0.9251
		NSi-CrossNPANI	0.9678	0.9212
	SE	NSi-NPANI	6.105673	9.490303
		NSi-CrossNPANI	8.48261	4.94961
	RMSE	NSi-NPANI	11.90664	25.35911
		NSi-CrossNPANI	12.17964	30.7296
	NSD	NSi-NPANI	14.64334	13.9302
		NSi-CrossNPANI	18.34884	13.09909
	ARE	NSi-NPANI	12.49533	13.57139
		NSi-CrossNPANI	15.51948	9.937769
	EBAS	NSi-NPANI	57.87569	120.9385
		NSi-CrossNPANI	63.83405	124.5767
	HYBRID	NSi-NPANI	235.6691	468.4501
		NSi-CrossNPANI	297.2514	580.922
	X^2	NSi-NPANI	9.85967	21.86136
		NSi-CrossNPANI	13.81224	30.97763
Sips	Q_{max} (mg g^{-1})	NSi-NPANI	117.4091	214.87379
		NSi-CrossNPANI	120.7976	380.9699
	K_s (L g^{-1})	NSi-NPANI	1.52×10^{-4}	4.60×10^{-5}
		NSi-CrossNPANI	1.01×10^{-6}	1.24×10^{-6}
	N	NSi-NPANI	0.988	0.945
		NSi-CrossNPANI	0.559	0.6569
	R^2	NSi-NPANI	0.9971	0.9969
		NSi-CrossNPANI	0.9409	0.9885
	SE	NSi-NPANI	0.692535	1.935586
		NSi-CrossNPANI	0.62397142	21.7881154
	RMSE	NSi-NPANI	17.03625	36.68615
		NSi-CrossNPANI	10.8533	42.34494
	NSD	NSi-NPANI	22.61605	34.37286
		NSi-CrossNPANI	14.11028	25.01729
	ARE	NSi-NPANI	14.53997	27.68759
		NSi-CrossNPANI	11.54116	20.12688
	EBAS	NSi-NPANI	70.33229	167.1095
		NSi-CrossNPANI	52.96363	230.8914
	HYBRID	NSi-NPANI	423.9456	2083.321
		NSi-CrossNPANI	176.267	1387.883
	X^2	NSi-NPANI	17.70307	50.77497
		NSi-CrossNPANI	8.817359	42.38072

Table 3 Isotherm parameters and error obtained by nonlinear fitting (three-parameter isotherm models) using NSi-NPANI and NSi-CrossNPANI

represent multilinearity forms and this refers to two or extra steps may occur. The first is indicating that the sharper portion of the line and attributed to the diffusion of divalent ions from the solution to the external surface of nano-crosslinked or the boundary strata diffusion of solute molecules or ions. The second portion is used to describe the gradual adsorption stage, where intraparticle diffusion is acting as the rate limiting [42–44].

Table 4 Isotherm parameters obtained by linear (two- and three-parameter isotherm models) using [NSi-NPANI] and [NSi-CrossNPANI]

| Model isotherm	Constants and error function	Nanocomposite	Metal ion	
			Cadmium	Lead
Langmuir	q_{max} (mg g^{-1})	NSi-NPANI	132.39	340.68
		NSi-CrossNPANI	164.75	761.23
	K_L (L mg^{-1})	NSi-NPANI	1.82×10^{-4}	3.97×10^{-5}
		NSi-CrossNPANI	2.15×10^{-4}	3.82×10^{-5}
	R^2	NSi-NPANI	0.9645	0.9848
		NSi-CrossNPANI	0.9276	0.9954
Freundlich	K_F (L mg^{-1})	NSi-NPANI	4.41×10^{-1}	7.48×10^{-2}
		NSi-CrossNPANI	1.56×10^{0}	1.79×10^{-1}
	n	NSi-NPANI	1.77	1.3
		NSi-CrossNPANI	2.21	1.35
	R^2	NSi-NPANI	0.95	0.9781
		NSi-CrossNPANI	0.8939	0.9799
Temkin	b_T	NSi-NPANI	69.07	30.3
		NSi-CrossNPANI	78.56	19.25
	A_T (L g^{-1})	NSi-NPANI	1.25×10^{-3}	4.13×10^{-4}
		NSi-CrossNPANI	2.88×10^{-3}	5.26×10^{-4}
	R^2	NSi-NPANI	0.8567	0.9758
		NSi-CrossNPANI	0.9678	0.9643
Dubinin-Radushkevich	q_s (mg g^{-1})	NSi-NPANI	90.86	162.04
		NSi-CrossNPANI	109.89	289.1
	K_{ads} (mol^2/KJ^2)	NSi-NPANI	2.99×10^{-1}	1.788
		NSi-CrossNPANI	2.60×10^{-1}	1.56
	R^2	NSi-NPANI	0.7263	0.704
		NSi-CrossNPANI	0.9467	0.7884
Redlish-peterson	K_R (L g^{-1})	NSi-NPANI	0.5	1.15
		NSi-CrossNPANI	1.7	0.29
	a_R (L mg^{-1})	NSi-NPANI	1.0133	14.987
		NSi-CrossNPANI	1.0274	1.3203
	b_R	NSi-NPANI	0.4438	0.2333
		NSi-CrossNPANI	0.5518	0.2735
	R^2	NSi-NPANI	0.918	0.8026
		NSi-CrossNPANI	0.9243	0.8566
Sips	Q_{max} (mg g^{-1})	NSi-NPANI	130.81	203.82
		NSi-CrossNPANI	118.54	334.69
	K_s (L g^{-1})	NSi-NPANI	5.84×10^{-5}	5.17×10^{-6}
		NSi-CrossNPANI	1.26×10^{-6}	1.21×10^{-6}
	n	NSi-NPANI	0.99	0.75
		NSi-CrossNPANI	0.56	0.65
	R^2	NSi-NPANI	0.9651	0.9656
		NSi-CrossNPANI	0.977	0.9709

The sorption of cadmium onto [NSi-NPANI] and [NSi-CrossNPANI] via the K_{id} value was identified as 15.04 and 18.451 mg g^{-1} min$^{-1/2}$ with R^2 equal 0.9677 and 0.9386, respectively. The value of C (2.0086 and 14.619 mg g^{-1}), gives an information about the thickness of the boundary layer. The greater the intercept, the larger is the boundary strata impact [42]. The aberration of the straight lines from the origin may be due to the diversity in the rate of mass transfer in the starting and eventual stages of adsorption. Further, such deviation of the straight lines from the origin refers to the pore dispersion is not alone rate controlling step [43]. Moreover, adsorption of two divalent ions onto two nanocomposites may proceed with two different steps. The first linear fraction was regarded to the surface adsorption or speedy external diffusion stage. The second linear portion is based on the piecemeal adsorption step

Table 5 Adsorption kinetic models for removal of different metal ion onto [NSi-NPANI] and [NSi-CrossNPANI]

Kinetic model	Constants	Nanocomposite	Metal ion	
			Cadmium	Lead
Pseudo-first order	q_e (mg g^{-1})	NSi-NPANI	114.93	157.54
		NSi-CrossNPANI	94.7	393.82
	K_1 (min^{-1})	NSi-NPANI	7.95×10^{-2}	8.63×10^{-2}
		NSi-CrossNPANI	7.16×10^{-2}	1.11×10^{-1}
	R^2	NSi-NPANI	0.9717	0.9845
		NSi-CrossNPANI	0.9847	0.9607
Pseudo-second order	q_e (mg g^{-1})	NSi-NPANI	102.04	175.4
		NSi-CrossNPANI	125	303.03
	K_2 (g mg^{-1} min^{-1})	NSi-NPANI	1.14×10^{-3}	1.67×10^{-3}
		NSi-CrossNPANI	1.54×10^{-4}	6.5×10^{-4}
	R^2	NSi-NPANI	0.9827	0.9887
		NSi-CrossNPANI	0.9915	0.9879
Intraparticle diffusion	K_{id} (mg g^{-1} min$^{-1/2}$)	NSi-NPANI	15.042	43.84
		NSi-CrossNPANI	18.451	21.943
	C	NSi-NPANI	2.0086	40.365
		NSi-CrossNPANI	14.619	48.22
	R^2	NSi-NPANI	0.9677	0.9858
		NSi-CrossNPANI	0.9386	0.9777
Elovich	α (mg g^{-1} min^{-1})	NSi-NPANI	83.022	163.73
		NSi-CrossNPANI	61.84	217.525
	β (g mg^{-1})	NSi-NPANI	1.08×10^{-1}	1.71×10^{-2}
		NSi-CrossNPANI	3.90×10^{-2}	3.39×10^{-2}
	R^2	NSi-NPANI	0.9826	0.9834
		NSi-CrossNPANI	0.9912	0.9877

Fig. 5 *Pseudo*-second order of lead and cadmium
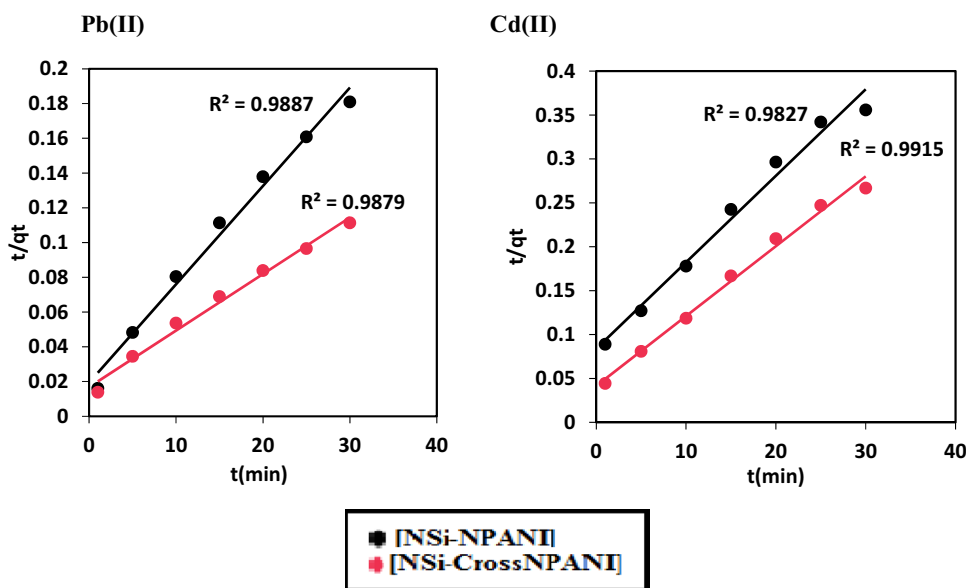
controlled by intra-particle-diffusion [45]. The sorption of metal ion on [NSi-NPANI] and [NSi-CrossNPANI] did not obey the intraparticle diffusion equation due to small R^2 values.

Table 5 showed that the *Elvoich* model constants obtained from plot (q_t) versus (ln t) for sorption of the two investigated metal ions. According to the Elovich model, the chemical reaction of divalent ions with the adsorbent

surface is known as the rate-controlling step (RCS) and the removal process takes place through a multilayer adsorption [46]. The Elovich parameters (α) for the adsorption initial rate of (cadmium and lead) onto [NSi-NPANI] and [NSi-CrossNPANI] were characterized in the range of 361.840 to 217.525 mg g^{-1} min^{-1}. The value of β indicates that the number of sites available for adsorption was increasing from 3.39×10^{-2} to 0.1084 by disparate metal ions upon the two modified nanocomposites. A plot of q_t versus ln t shows that the sorption of metal ion on [NSi-NPANI] and [NSi-CrossNPANI] did not obey the Elovich equation due to small R^2 values.

The equilibrium adsorption and kinetic data assume that the surfaces of [NSi-NPANI] and [NSi-CrossNPANI] are homogeneous and therefore, the adsorption mechanism is chemisorption. The *pseudo* second-order equation is widely used to construe chemisorption of metal ion onto a homogeneous surface. In this work, different adsorption mechanisms of metal ions onto [NSi-NPANI] and [NSi-CrossNPANI] have been proposed. These involve surface adsorption, ion exchange, chemisorption and complexation. Ion exchange is the most prevalent mechanism by the reaction of metal ions with surface functional groups of silica-loaded nanopolyaniline such as the silanol groups. The chemisorptive reaction could be formed by participation a pair of electrons of nitrogen atoms with metal ions. Surface adsorption is another mechanism by which metal ions may be bound to [NSi-NPANI] or [NSi-CrossNPANI]. This mechanism is a surface reaction where a positively charged cadmium or lead ion was attracted to a negatively charged surface of nano-crosslinked without the exchange of ions or electrons. The possible mechanism of metal binding with [NSi-NPANI] is represented in Scheme 3.

Thermodynamic Studies

The impact of temperature on adsorption of metal ions (cadmium and lead) by [NSi-NPANI] and [NSi-CrossNPANI] was studied. (ΔG^o), (ΔH^o) and (ΔS^o) are generally calculated to discuss the adsorption operations and these are represented by the variation in standard enthalpy. These parameters are estimated from Eq. 3 as previously reported [47].

$$\ln(55.5 b_M) = -\frac{\Delta G}{RT} = \frac{\Delta S}{R} - \frac{\Delta H}{RT} \tag{3}$$

where b_M is the Langmuir equilibrium (L mol^{-1}), ΔG^o is the standard free energy change of sorption (kJ mol^{-1}), T is the temperature in (K), R is the real gas constant (8.314J mol^{-1}K^{-1}), ΔH^o is the standard enthalpy change (kJ mol^{-1}) and ΔS^o is standard entropy change (kJ mol^{-1} K^{-1}). In this work, the values of ln (55.5b_M) were sketched against 1/T as shown in Fig. 6, from which the ΔH^o and ΔS^o values can be appraised from the slope and intercept. The calculated (ΔH^o), (ΔS^o), and (ΔG^o) are collected in Table S5 (Supplementary materials).

The characterized sign of ΔG^o values was negative at all temperatures revealing the spontaneous nature of these adsorptions. The ΔG^o values were also found to decrease as T increases, indicating a less driving force for adsorption at higher T. Generally, the ΔG^o results are near to each other indicating that such spontaneity is independent on T. Moreover, the adsorption operations are exothermic according to negative sign of ΔH^o. As previously reported, the magnitude of ΔH^o value in the range of 2.1–20.9 kJ/mol (physical adsorption) and 80–200 kJ/mol (chemical

Fig. 6 Plot of ln (55.5b_M) versus 1/T for the adsorption of [NSi-NPANI] and [NSi-CrossNPANI]

[NSi-NPANI]
[NSi-CrossNPANI]
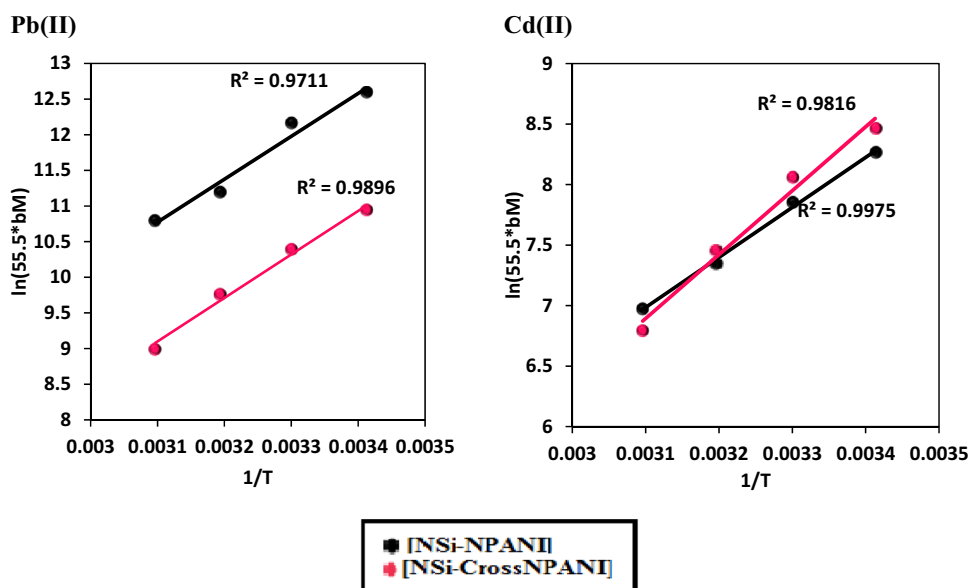
adsorption) reactions may be outlined [48]. In this work, the ΔH^o value is larger than 20.9 kJ/mol and this indicates the chemical adsorption of metal ions onto [NSi-NPANI] and [NSi-CrossNPANI]. Finally, the negative ΔS^o values correspond to the organization of the adsorbed species becomes less random and suggest the decrease in concentration of ions in solid-solution interface indicating thereby increase in divalent ions onto the nanocrosslinked solid phase. This is the normal effect of the chemical adsorption process, which takes place through chemisorptive interactions [48].

Desorption and Reusability Study

Regeneration of used nanocomposite is an important operation from the economical point of vision [49]. In this work, nanocomposites-bound-metal ions were subjected to regeneration by shaking with 0.1 mol L^{-1} of HCl for 2 min at room temperature. The recycled nanocomposites were filtered, repeatedly washed with distilled water till acid-free and finally dried at 60 °C. The regenerated nano-crosslinked nanocomposites were then used for removal of heavy metal ions from aqueous solution to identify the metal capacity values and percentage of stability in acid solution. The recycled nanocomposites were found to maintain 94.1–100.0% of their reactivity toward the removal of metal ions. Thus, the designed nanocomposites in this work were characterized by their high stability and therefore they can be used several times without decreasing the adsorption capacities significantly.

Adsorptive Removal of Metal Ions Using Multi-Stage Micro-Column Technique

The potential implementation of newly designed nanocomposites, [NSi-NPANI] and [NSi-CrossNPANI] for adsorptive removal of cadmium and lead from various water specimens (tap water, sea water and industrial wastewater) were explored using a multistage micro-column technique. The identified % recovery values are collected in Table 6. The percentage extraction values of lead using [NSi-NPANI] nanocomposite as the packing material were identified as 100.0% from tap water, 93.0% from industrial wastewater and 70.2% for sea water via the third extraction step. In addition, the extraction of lead from different water samples using [NSi-CrossNPANI] were identified as 98.5% (tap water) via second extraction step and 91.9% (industrial

Table 6 Adsorptive removal of different metal ions from water samples by [NSi-NPANI] and [NSi-CrossNPANI]

Nanocomposite	Metal ion	Percentage extraction (%) of metal ions from water samples*		
		Wastewater	Sea water	Tap water
NSi-CrossNPANI	Cadmium	89.9	50.1	90.8
	Lead	91.9	65.7	98.5
NSi-NPANI	Cadmium	78.7	33.8	92.4
	Lead	93	70.2	100
NSi	Cadmium	67.6	15.8	70.5
	Lead	75	36.8	81

*Percentage extraction values are based on triplicate measurements ± 3.0%

wastewater) via third extraction step and 65.7% (sea water) via third extraction step. The adsorptive removal of cadmium using [NSi-NPANI] was identified to produce 92.4% (tap water), 78.7% (industrial wastewater) and 33.8% (sea water) using third extraction step. The cadmium removal by [NSi-CrossNPANI] as the packing material was identified as 90.8% and 89.9% from tap water and industrial wastewater specimens, respectively.

Conclusion

The current work provides a simple and green process for synthesis of two novel modified silica nanocomposites based on the functionalization of nanosilica (NSi) with NPANI and CrossNPANI. The optimum extraction conditions of metal ions were found in the range pH 6.0–7.0. It was concluded that both nonlinear and linear regression analyses exhibited better performance with respect to the Langmuir and sips models describing the best adsorption operation. In addition, the linear regression analysis by the three-parameter model was always found to provide a better match with the experimental data for cadmium than the two-parameter model. The nonlinear regression analysis of Langmuir isotherm was better fitted with the data of lead and cadmium onto the two nanocomposites. The adsorptive extraction of lead from tap water and wastewater was successively accomplished with 98.5–100.0 and 91.9–93.0%, respectively. Finally, the advantages of newly functionalized nanocomposites were compared with some previously reported adsorbents [45–51] as listed out in Table 7.

Table 7 Comparison of the proposed nano-sorbents with other published similar materials

Sorbent	Adsorbate	Adsorption studies and Data	Ref.
Polyaniline coated on saw dust (PANI/SD)	Cd(II)	The maximum metal capacity of Cd(II) was 500 mg g^{-1}at pH 6	[50]
Chitosan and polyaniline graft chitosan beads (PGCB)	Cu(II)	The maximum adsorption capacity was 52.6–100 mg g^{-1} at a solution pH 5	[51]
Polyaniline grafted chitosan (PGC)	Cd(II), Pb(II)	The maximum monolayer capacity obtained from the Langmuir isotherm was 16.07 and 14.33 mg g^{-1} for Pb(II) and Cd(II) ions, respectively	[52]
Polyaniline coated on saw dust (PANi/SD)	Cd(II), Pb(II) and Hg(II)	The maximum adsorption capacity was 3.4 mg g^{-1}. Sorption/desorption of lead ions by PANi, is mostly reversible and the processes can be simply controlled by pH of solution	[53]
Polyaniline/palygorskite (PP) composite	Cu(II), Ni(II), Cd(II), and Cr(VI)	The adsorption capacity were 114, 84, 56 and 198 mg g^{-1} Cu(II), Ni(II), Cd(II) and Cr (VI), respectively	[54]
Humic acid-polyaniline systems(HA-PEB)	Cd(II), Zn(II) and Ni(II)	Batch adsorption results showed that q$_{max}$ of Cd(II), Zn(II) and Ni(II) on HA-PEB followed the order: THA-PEB > YHA-PEB > PFHA-PEB	[55]
PANI/ multiwalled carbon nanotubes (MWC-NTs) magnetic composites	Pb(II)	The maximum capacity for Langmuir model are 12.6 mg g^{-1} for MWCNTs, ~ 13.3 mg g^{-1} for MWCNTs-treat, ~21.0 mg g^{-1} for PANI, and ~22.2 mg g^{-1} for PANI/ MWCNTs under the experimental conditions	[56]
[NSi-NPANI] and [NSi-CrossNPANI]	Cd(II) and Pb(II)	The results of this study showed that nonlinear Langmuir and sips models were the best fit than others	This work
		The kinetic study revealed that the pseudo-second order kinetic model was the best model to explain the kinetic data for Cd(II) and Pb(II)	
		Thermodynamic parameters were calculated	
		Q$_{max}$ values are 91.8 to 112.4 and 165.8 to 279.9 mg g^{-1} for Cd(II) and Pb(II) in pH 6–7, respectively	
		The recycled nanosorbents were found to maintain 94.1–100.0% of their reactivity toward removal of metal ions	

References

1. Ghobashy MM, Khafaga MR (2017) Chemical modification of nano polyacrylonitrile prepared by emulsion polymerization induced by gamma radiation and their use for removal of some metal ions. J Polym Environ 25:343–348
2. Gupta VK, Ali I (2012) Environmental water: advances in treatment, remediation and recycling. Elsevier, The Netherlands, ISBN: 978-0-444-59399-3
3. Ali I, Aboul-Enein HY (2006) Instrumental methods in metal ions speciation: chromatography, capillary electrophoresis and electrochemistry. Taylor and Francis Ltd., New York, ISBN: 0-8493-3736-4
4. Ali I, Aboul-Enein HY, Gupta VK (2009) Nano chromatography and capillary electrophoresis: pharmaceutical and environmental analyses. Wiley, Hoboken, ISBN: 978-0-470-17851-5
5. Dehghani MH, Sanaei D, Ali I, Bhatnagar A (2016) Removal of chromium(VI) from aqueous solution using treated waste newspaper as a low-cost adsorbent: kinetic modeling and isotherm studies. J Mol Liq 215:671–679
6. Ali I, Jain CK (2004) Advances in arsenic speciation techniques. Int J Environ Anal Chem 84:947–964
7. Al-Hussaini AS, Elias M, Abd El-Ghaffar AM (2017) A new poly(aniline-co-o-phenylenediamine)/kaolinite microcomposites for water decontamination. J Polym Environ 25:35–45
8. Elsherbiny AS, El-Hefnawy ME, Gemea AH (2018) Adsorption efficiency of polyaspartate-montmorillonite composite towards the removal of Pb(II) and Cd(II) from aqueous solution. J Polym Environ. https://doi.org/10.1007/s10924-017-0958-9
9. Mallakpour S, Nouruzi N (2018) Application of vitamin B1-coated carbon nanotubes for the production of starch nanocomposites with enhanced structural, optical, thermal and

Cd(II) adsorption properties. J Polym Environ. https://doi.org/10.1007/s10924-018-1177-8

10. Mahmoud ME, Yakout AA, Hussein KH, Osman MM (2015) Magnetic accumulation and extraction of Cd(II), Hg(II) and Pb(II) by a novel nano-Fe_3O_4-coated-dioctylphthalate-immobilized-hydroxylamine. J Environ Chem Eng 3:843–851

11. Mahmoud ME, Abdou AE, Nabil GM (2015) Facile microwave-assisted fabrication of nano-zirconium silicate-functionalized-3-aminopropyltrimethoxysilane as a novel adsorbent for superior removal of divalent ions. J Ind Eng Chem 32:365–372

12. Vakili M, Rafatullah M, Salamatinia B et al (2014) Application of chitosan and its derivatives as adsorbents for dye removal from water and wastewater: a review. Carbohydr Polym 113:115–130

13. Ćirić-Marjanović G (2013) Recent advances in polyaniline research: polymerization mechanisms, structural aspects, properties and applications. Synth Met 177:1–47

14. Abbas A, Al-Amer AM, Laoui T (2016) Heavy metal removal from aqueous solution by advanced carbon nanotubes: critical review of adsorption applications. Sep Purif Technol 157:141–161

15. Bushra R, Naushad M, Adnan R et al (2015) Polyaniline supported nanocomposite cation exchanger: synthesis, characterization and applications for the efficient removal of Pb^{2+} ion from aqueous medium. J Ind Eng Chem 21:1112–1118

16. Javadian H, Sorkhrodi FZ, Koutenaei BB (2014) Experimental investigation on enhancing aqueous cadmium removal via nanostructure composite of modified hexagonal type mesoporous silica with polyaniline/polypyrrole nanoparticles. J Ind Eng Chem 20:3678–3688

17. Khan AA, Shaheen S (2015) Preparation, characterization and kinetics of ion exchange studies of Ni^{2+} selective polyaniline–Zr(IV) molybdophosphate nanocomposite cation exchanger. J Ind Eng Chem 26:157–166

18. Javadian H (2014) Application of kinetic, isotherm and thermodynamic models for the adsorption of Co(II) ions on polyaniline/polypyrrole copolymer nanofibers from aqueous solution. J Ind Eng Chem 20:4233–4241

19. Moazezi N, Moosavian MA (2016) Removal of rubidium ions by polyaniline nanocomposites modified with cobalt-Prussian blue analogues. J Environ Chem Eng 4:2440–2449

20. Bhaumik M, Noubactep C, Gupta VK et al (2015) Polyaniline/Fe 0 composite nanofibers: an excellent adsorbent for the removal of arsenic from aqueous solutions. Chem Eng J 271:135–146

21. Janaki V, Vijayaraghavan K, Oh BT (2012) Starch/polyaniline nanocomposite for enhanced removal of reactive dyes from synthetic effluent. Carbohydr Polym 90:1437–1444

22. Zhou Q, Wang Y, Xiao J, Fan H (2016) Adsorption and removal of bisphenol A, α-naphthol and β-naphthol from aqueous solution by Fe_3O_4@ polyaniline core–shell nanomaterials. Synth Met 212:113–122

23. Ballav N, Debnath S, Pillay K, Maity A (2015) Efficient removal of reactive black from aqueous solution using polyaniline coated ligno-cellulose composite as a potential adsorbent. J Mol Liq 209:387–396

24. Gemeay AH, Elsharkawy RG, Aboelfetoh EF (2018) Graphene oxide/polyaniline/manganese oxide ternary nanocomposites, facile synthesis, characterization, and application for indigo carmine removal. J Polym Environ. https://doi.org/10.1007/s10924-017-0947-z

25. Mahmoud ME, Fekry NA, El-Latif MM (2016) Nanocomposites of nanosilica-immobilized-nanopolyaniline and crosslinked nanopolyaniline for removal of heavy metals. Chem Eng J. 304:679–691

26. Janaki V, Vijayaraghavan K, Ramasamy A et al (2012) Competitive adsorption of reactive orange 16 and reactive brilliant blue R on polyaniline/bacterial extracellular polysaccharides composite—a novel eco-friendly polymer. J Hazard Mater 241:110–117

27. Janaki V, Oh BT, Shanthi K et al (2012) Polyaniline/chitosan composite: an eco-friendly polymer for enhanced removal of dyes from aqueous solution. Synth Met 162:974–980

28. Nagy B, Mânzatu C, Măicăneanu A et al (2014) Linear and nonlinear regression analysis for heavy metals removal using *Agaricus bisporus* macrofungus. Arab J Chem. ISSN: 1878–5352

29. Kumara N, Hamdan N, Petra MI et al (2014) Equilibrium Isotherm studies of adsorption of pigments extracted from Kuduk-kuduk (*Melastoma malabathricum* L.) pulp onto TiO_2 nanoparticles. Hindawi J Chem 2014

30. Chen X (2015) Modeling of experimental adsorption isotherm data. Inform J 6:14–22

31. Amrhar O, Nassali H, Elyoubi MS (2015) Two and three-parameter isothermal modeling for adsorption of crystal violet dye onto natural illitic clay: nonlinear regression analysis. J Chem Pharm Res 7:892–903

32. Butnariu M, Negrea P, Lupa L et al (2015) Remediation of rare earth element pollutants by sorption process using organic natural sorbents. Int J Environ Res Publ Health 12:11278–11287

33. Ayad M, Zaghlol S (2012) Nanostructured crosslinked polyaniline with high surface area: synthesis, characterization and adsorption for organic dye. Chem Eng J 204:79–86

34. Javadian H, Ghaemy M, Taghavi M (2014) Adsorption kinetics, isotherm, and thermodynamics of Hg^{2+} to polyaniline/hexagonal mesoporous silica nanocomposite in water/wastewater. J Mater Sci 49:232–242

35. Anbazhagan S, Alagar M, Gnanasundaram P (2011) Synthesis and characterization of organic-inorganic hybrid clay filled and bismaleimide—siloxane modified epoxy nanocomposites. J Plast Technol 15:30–45

36. Hongxia Z, Xiaoyun W, Honghong L et al (2016) Adsorption behavior of Th(IV) onto illite: effect of contact time, pH value, ionic strength, humic acid and temperature. Appl Clay Sci 127:35–43

37. Wang X, Wang C (2016) Chitosan-poly (vinyl alcohol)/attapulgite nanocomposites for copper (II) ions removal: pH dependence and adsorption mechanisms. Coll Surf 500:186–194

38. Wiśniewska M, Chibowski S, Urban T (2016) Adsorption properties of the nanozirconia/anionic polyacrylamide system—effects of surfactant presence, solution pH and polymer carboxyl groups content. Appl Surf Sci 370:351–356

39. Mahmoud ME, Ahmed SB, Osman MM, Abdel-Fattah TM (2015) A novel composite of nanomagnetite-immobilized-baker's yeast on the surface of activated carbon for magnetic solid phase extraction of Hg(II). Fuel 139:614–621

40. Mondal P, Balomajumder C, Mohanty B (2007) A laboratory study for the treatment of arsenic, iron, and manganese bearing ground water using Fe^{3+} impregnated activated carbon: effects of shaking time, pH and temperature. J Hazard Mater 144:420–426

41. Hossain M, Ngo H, Guo W (2013) Introductory of microsoft excel SOLVER function-spreadsheet method for isotherm and kinetics modelling of metals biosorption in water and wastewater. J W S 3:223–237

42. Bany-Aiesh H, Banat R, Al-Sou'od K (2015) Kinetics and adsorption isotherm of ibuprofen onto grafted β-CD/Chitosan polymer. Am J Appl Sci 12:917

43. Srivastava P, Hasan SH (2011) Biomass of *Mucor heimalis* for the biosorption of cadmium from aqueous solutions: equilibrium and kinetic studies. BioRes 6:3656–3675

44. Dawodu FA, Akpomie KG (2014) Kinetic, equilibrium, and thermodynamic studies on the adsorption of cadmium(II) ions using "Aloji Kaolinite" mineral. Pac J Sci Technol 15:268–276

45. Belhachemi M, Addoun F (2012) Adsorption of congo red onto activated carbons having different surface properties: studies

of kinetics and adsorption equilibrium. Desalin Water Treat J 37:122–129

46. Hosseini-Bandegharaei A, Khamirchi R, Hekmat-Shoar R et al (2016) Sorption efficiency of three novel extractant-impregnated resins containing vesuvin towards Pb(II) ion: effect of nitrate and amine functionalization of resin backbone. Colloids Surf A Physicochem Eng Asp 504:62–74

47. Rahmani-Sani A, Shan R, Yan L, Hosseini-Bandegharaei A (2017) Response to" Letter to Editor: minor correction to the thermodynamic calculation using the distribution constant by Shan et al. and Rahmani-Sani et al. J Hazard Mater 325:367

48. Sheela T, Nayaka YA, Viswanatha R et al (2012) Kinetics and thermodynamics studies on the adsorption of Zn(II), Cd(II) and Hg(II) from aqueous solution using zinc oxide nanoparticles. Powder Technol 217:163–170

49. Hosseini-Bandegharaei A, Karimzadeh M, Sarwghadi M et al (2014) Use of a selective extractant-impregnated resin for removal of Pb(II) ion from waters and wastewaters: kinetics, equilibrium and thermodynamic study. Chem Eng Res Des 92:581–591

50. Mansour MS, Ossman ME, Farag HA (2011) Removal of Cd(II) ion from waste water by adsorption onto polyaniline coated on sawdust. Desalination 272:301–305

51. Igberase E, Ofomaja A (2014) The adsorption of copper(II) ions by polyaniline graft chitosan beads from aqueous solution: equilibrium, kinetic and desorption studies. J Environ Chem Eng 2:362–369

52. Karthik R, Meenakshi S (2014) Removal of Pb(II) and Cd(II) ions from aqueous solution using polyaniline grafted chitosan. Chem Eng J 263:168–177

53. Ansari R, Raofie F (2006) Removal of lead ion from aqueous solutions using sawdust coated by polyaniline. E-J Chem 3:49–59

54. Kong Y, Wei J, Wang Z et al (2011) Heavy metals removal from solution by polyaniline/palygorskite composite. J Appl Polym Sci 122:2054–2059

55. Terbouche A, Ramdane-Terbouche CA, Hauchard D, Djebbar S (2011) Evaluation of adsorption capacities of humic acids extracted from Algerian soil on polyaniline for application to remove pollutants such as Cd(II), Zn(II) and Ni(II) and characterization with cavity microelectrode. J Environ Sci 23:1095–1103

56. Shao D, Chen C, Wang X (2012) Application of polyaniline and multiwalled carbon nanotube magnetic composites for removal of Pb (II). Chem Eng J 185:144–150